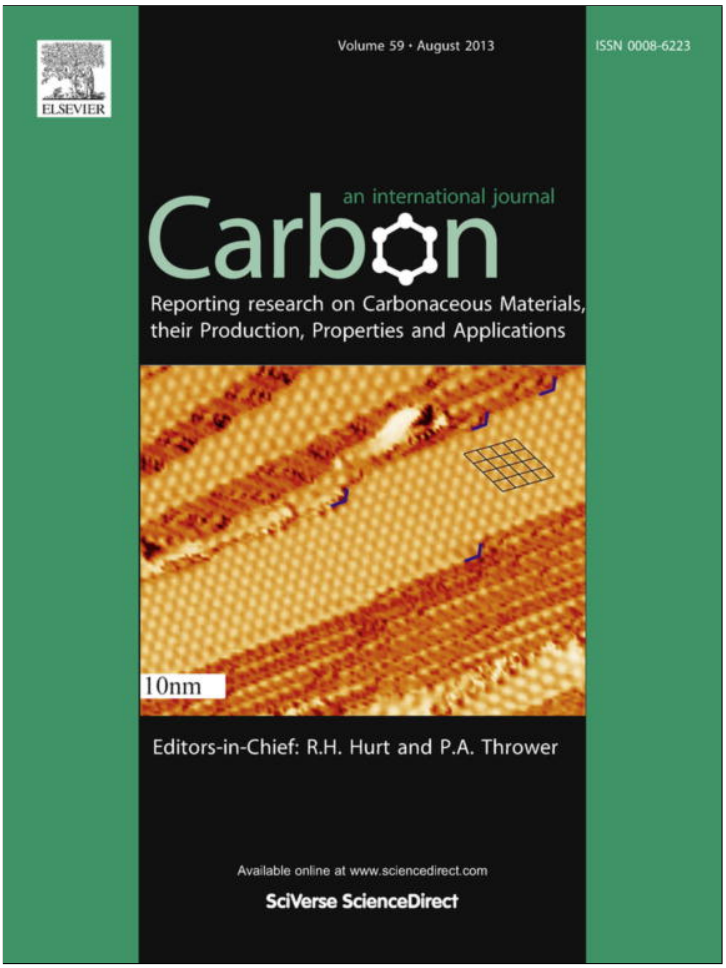

CARBON 59 (2013) 76–92

Available at www.sciencedirect.com

SciVerse ScienceDirect

journal homepage: www.elsevier.com/locate/carbon

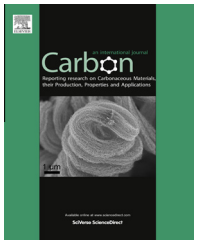

A ceramic–carbon hybrid as a high-temperature structural monolith and reinforcing filler and binder for carbon/carbon composites

Andi Wang, Xiaoqing Gao [1], *Rossman F. Giese Jr.* [2], *D.D.L. Chung* [*]

Composite Materials Research Laboratory University at Buffalo, State University of New York, Buffalo, NY 14260-4400, USA

ARTICLE INFO

Article history:
Received 4 January 2013
Accepted 23 February 2013
Available online 13 March 2013

ABSTRACT

A new ceramic–carbon nanostructured hybrid (86 vol.% ceramics, 14 vol.% carbon) formed from organoclay during pyrolysis is reported. It functions as a reinforcing filler and a binder for carbon/carbon (C/C) composites. Alone, it can also serve as a high-temperature structural monolith. During pyrolysis, the ordered montmorillonite clay (d_{001} 31.5 Å) is transformed to mullite, cristobalite and disordered clay, allowing the clay part of the organoclay to serve as both binder and reinforcement. The organic part serves as a binder. Thus, a unidirectional C/C composite (50 vol.% fibers, 33 vol.% carbon matrix, 5 vol.% hybrid and 12% porosity) exhibiting flexural strength 290 MPa, modulus 55 GPa and toughness 2.9 MPa is obtained by 1000 °C 21-MPa hot-press pyrolysis in the presence of mesophase pitch powder, which serves as an additional binder, without densification after the pyrolysis. With the hybrid incorporation, the fiber content decreases from 53 to 50 vol.%, but the flexural strength and modulus are increased by 46% and 14% respectively, relative to the composite without the hybrid but with densification. Hot pressing the organoclay alone forms a black monolithic sheet with high thermal stability, electrical resistivity 6×10^6 Ω cm, flexural strength 180 MPa, modulus 69 GPa, but low ductility.

1. Introduction

Carbon/carbon (C/C) composites are important as high-temperature lightweight structural materials, as used for reentry vehicles, missiles and aircraft brakes. In addition, they are valuable for biomedical and corrosion-resistant applications. However, they suffer from high processing cost, which is due to the need to use multiple impregnation-carbonization cycles and methods such as chemical vapor infiltration (CVI) in order to achieve sufficient densification and hence adequate mechanical properties. In addition, they suffer from low ductility, due to the brittleness of the carbon matrix.

The incorporation of partially exfoliated nanoclay in a C/C fabric composite (prepared by carbonization at 1000 °C, followed by densification) by the addition of the organoclay particles to cyanate ester resin (the carbon matrix precursor) improves slightly the oxidation resistance at elevated temperatures, while the true density is increased from 1.52 to 1.57 g/cm^3; the effect of the nanoclay incorporation on the

[*] *Corresponding author:* Fax: +1 716 645 2883.
E-mail address: ddlchung@buffalo.edu (D.D.L. Chung).
[1] Permanent address: Key Laboratory of Carbon Materials, Institute of Coal Chemistry, Chinese Academy of Sciences, 27 Taoyuan South Road, Taiyuan 030001, China.
[2] Also with Department of Geology, University at Buffalo, State University of New York.
0008-6223/$ - see front matter
http://dx.doi.org/10.1016/j.carbon.2013.02.057

mechanical properties was not reported [1]. The incorporation of SiC in a C/C composite by carbothermal reduction of SiO_2 to SiC (mainly SiC whiskers) decreases the flexural strength [2]. The incorporation of SiC whiskers in a C/C composite by the growth of the whiskers on a carbon fabric also decreases the flexural strength [3]. The incorporation of SiC in a C/C composite by liquid silicon infiltration increases the flexural strength from 82 to 120 MPa [4]. The incorporation of carbon black in a C/C composite increases the flexural strength from 15 to 42 MPa, in addition to increasing the true density from 1.52 to 1.67 g/cm^3 and decreasing the open porosity from 9% to 8% [5]. Filler incorporation is much less expensive than *in situ* filler growth. The incorporation of carbon nanotubes (CNT) in a C/C composite by *in situ* growth of CNT on the carbon fibers increases the flexural strength from 179 to 233 MPa and increases the flexural modulus from 33 to 58 GPa, in addition to increasing the true density [6]. The incorporation of carbon nanofibers in a C/C composite by mixing the nanofibers with the precursor resin has negligible effect on the interlaminar shear strength [7]. Thus, based on the limited amount of prior work, the effect of filler incorporation or growth on the mechanical properties of C/C composites can be positive or negative. Organoclay is particularly attractive due to its low cost compared to SiC whiskers, CNT and carbon nanofibers. In addition, organoclay is attractive for its organic component, which enhances the hydrophobicity of the clay [8]; the hydrophobic character is valuable due to the organic nature of the carbon matrix precursor. Furthermore, the structure of the C/C composites containing fillers has not received adequate attention. The situation calls for further investigation of both the structure and the properties.

Although organoclay has been investigated extensively for use as a filler in composite materials, particular polymer–matrix composites, it has not been previously explored for use as both a filler and a binder. This work has shown for the first time that organoclay can serve both functions at the same time in a carbon–matrix composite, such that the filler and binder functions stem from the inorganic part of the organoclay, whereas the binder function stems from the organic part of the organoclay. The organic part serves as a carbon precursor. The dual functions allow the organoclay to be highly effective for strengthening C/C composites, as shown for the first time in this work.

Although organoclay has been previously investigated as a filler in C/C composites [1], it has not been previously investigated as the sole ingredient in forming a monolithic material. This work has shown for the first time that the hot pressing of organoclay in the absence of any other ingredient results in a monolithic material, due to the binding ability of the organoclay. Furthermore, this monolithic material exhibits high flexural strength and modulus, as shown in this work, due to the reinforcing ability of the inorganic part of the organoclay.

This work is primarily aimed at (i) investigating the mechanical properties of C/C composites containing organoclay through filler incorporation and elucidating the structure of this multi-scale composite, (ii) investigating the feasibility and effect of conversion of the organic component of organoclay to carbon and the associated feasibility of forming a ceramic–carbon hybrid from organoclay in the absence of any other ingredient, (iii) investigating the feasibility of organoclay serving as both filler and binder at the same time, (iv) investigating the feasibility of using organoclay incorporation to facilitate the low-cost fabrication of C/C composites without densification, and (v) investigating the feasibility of using organoclay in the absence of any other ingredient to form a low-cost monolithic high-temperature structural material.

2. Experimental methods

2.1. Materials

Organically modified clay (called organoclay, also known as nanoclay) is manufactured by modifying clay with quaternary ammonium cations via a cation exchange process. The organoclay [9,10] used is a natural montmorillonite that has been intercalated with a quaternary ammonium salt (dimethyl, dihydrogenated tallow) with chloride anions. Montmorillonite constitutes 90% of the composition of an industrial grade bentonite. The basal spacing d_{001} = 31.5 Å, as shown by X-ray diffraction (XRD) in Fig. 1(a). The powder XRD was conducted with CuKα radiation (40 kV, 30 mA) using a Siemens Kristalloflex diffractometer equipped with a

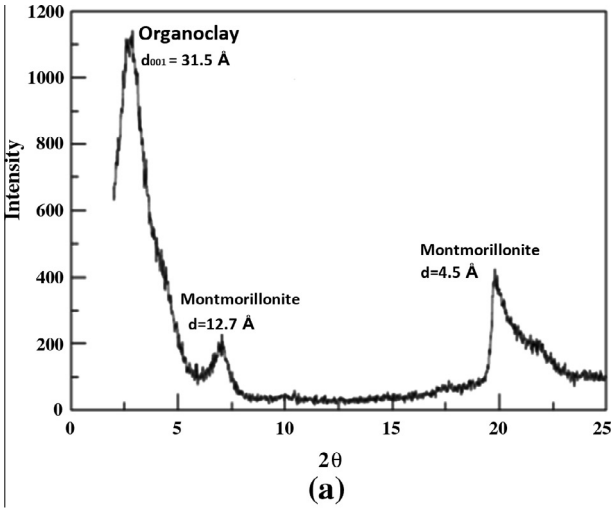

Fig. 1 – As-received organoclay (i.e., organoclay before hot pressing). (a) X-ray diffraction pattern. (b) SEM photograph showing feathery particles.

diffracted-beam graphite monochromator. The particles are white (more exactly, off white) and have a feathery morphology (Fig. 1(b)).

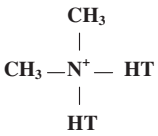

The hydrogenated tallow (abbreviated HT in the schematic above) in the ammonium cation involves ~65% fatty acids with 18 carbon atoms in the alkyl carbon chain in each molecule, ~30% fatty acids with 16 carbon atoms in the chain, and ~5% fatty acids with 14 carbon atoms in the chain. The cation exchange capacity is 125 cmol/kg. The true density of the organoclay is 1.66 g/cm^3. The loss on ignition is 43 wt.%. The particle size is such that 10% is less than 2 μm, 50% is less than 6 μm and 90% is less than 13 μm. Phyllosilicates are inherently hydrophilic, but ion exchange involving the cations in the silicate and the ammonium salt renders the clay more hydrophobic. The organoclay has a reduced surface energy, which is well-suited for use with organic matrices. The layered magnesium aluminum silicate platelets in an organoclay particle are 1 nm thick and 70–150 nm across, with an aspect ratio 70–150 and a surface area exceeding 750 m^2/g [11]. This organoclay is the product designated Cloisite 15A, as provided by Southern Clay Products, Inc., Gonzales, TX.

There are two main classes of bentonite, based on the dominant exchangeable ion that is weakly bound in the interlayer of montmorillonite. They are sodium bentonite and calcium bentonite. Sodium bentonite swells more in water than calcium bentonite and has excellent colloidal properties. For the sake of comparison, clay without an organic component is also used, namely sodium bentonite (Asbury Graphite Mills, Inc., Asbury, NJ, M325). It contains 2–6% free SiO_2 and has less than 10% moisture. It has a cation exchange capacity (CEC) 92 cmol/kg, true density 2 g/cm^3 and negligible solubility in water; 98.65% of the powder passes through U.S. 325 mesh (corresponding to 44 μm).

The continuous carbon fibers are Thornel P-25X mesophase-pitch-based fibers (without sizing and without twist) from Cytec Industries Inc, Woodland Park, NJ. It is in the form of 2000-filament tows, with tensile strength 1.56 GPa, tensile modulus 159 GPa, true density 1.92 g/cm^3, diameter 10 μm and carbon content 97+%.

The pitch used as the carbon matrix precursor for both the composite fabrication and the subsequent optional densification process is mesophase pitch powder (coal tar pitch, with average particle size 20 μm, softening temperature slightly above 300 °C and coking value 0.8) from Koppers Inc., Pittsburgh, PA. The dispersant for dispersing the pitch in water is poly(ethylene oxide) (PEO), a water soluble resin powder (UCARFLOC Polymer 310, Dow Chemical Co, Midland, MI).

2.2. Composite fabrication

The organoclay and pitch powder in the mass ratio of 1:4 are dry mixed in a ball mill (without grinding balls) for 24 h for the purpose of initial mixing. Then the mixture is dispersed in water that contains 0.1 wt.% dissolved PEO, such that the dispersion contains 10 wt.% organoclay-pitch mixture. The dispersion is stirred manually for 10–20 min, followed by 2.0 h of magnetic stirring, in order to achieve an adequate degree of mixing. The carbon fiber tow is immersed in the dispersion for 3.0 h in order for the tow to be coated with the organoclay-pitch mixture.

The mass ratio of the immersed fibers to pitch (in the dispersion) to organoclay (also in the dispersion) is 50:40:10. This proportion is such that the entirety of the liquid-based dispersion is consumed in coating the immersed fibers. Thus, the mass ratio of the fibers to pitch to organoclay in the prepreg is also 50:40:10. In other words, the prepreg contains 50 wt.% fibers, 40 wt.% pitch and 10 wt.% organoclay.

After removal of the tow from the dispersion, the tow is placed on a piece of Teflon (polytetrafluoroethylene) sheet, such that 17 tows are manually aligned to form a prepreg sheet of size 290 × 38 mm. Multiple sheets are made.

After this, the prepreg sheets are cut into discs of diameter 31.8 mm. A total of 8 discs are then unidirectionally stacked to form a cylinder. The stacked discs are allowed to dry in air at room temperature, followed by hot pressing in a graphite mold under a nitrogen purge at a flow of 70 ml/min for the purpose of pyrolysis (carbonization). The temperature is first raised from room temperature (20 °C) to 300 °C in a period of 1.0 h without pressure application, such that the heating rate is constant. After this, the temperature is increased from 300 to 700 °C over a period of 1.0 h at a uniaxial pressure of 21 MPa, such that the heating rate is constant. Then the temperature is increased from 700 to 1000 °C over a period of 1.0 h at the same pressure, such that the heating rate is constant. Finally the temperature is maintained at 1000 °C for 30 min at the same pressure. After this, cooling is conducted naturally in the furnace under nitrogen, which is maintained until the temperature has reached 300 °C. Imperfect alignment of the carbon fibers necessarily occurs to a degree in all the composites of this work.

One cycle of densification in the form of pitch impregnation and recarbonization is optionally conducted for the C/C composite without a filler. However, densification is not conducted for the composite with filler. In the impregnation, 1.00 g of pitch powder is placed below the carbonized composite in the graphite mold and another 1.00 g of pitch powder is placed above it. The sandwich is then heated to 360 °C at 5 °C/min at an applied pressure of 5 MPa at temperatures from 300 to 360 °C. Upon reaching 360 °C, a pressure of 10.0 MPa is applied. The highest temperature of 360 °C is maintained for 2.0 h under the pressure of 10.0 MPa. After the impregnated sandwich has been cooled (within the furnace without an applied pressure) to 300 °C, it is immediately reheated to 1000 °C at 6 °C/min under a pressure of 16 MPa for the purpose of recarbonization. The highest temperature of 1000 °C is maintained for 30 min under the pressure of 16 MPa. Purging nitrogen gas at a flow of 70 ml/min is applied throughout the impregnation and recarbonization process. After cooling to room temperature, the excessive carbonized pitch is detached from the composite specimen.

2.3. Hot pressing clays in the absence of the pitch or the carbon fibers

In order to investigate the response of the clay to hot pressing (which is under the same conditions as in carbonization,

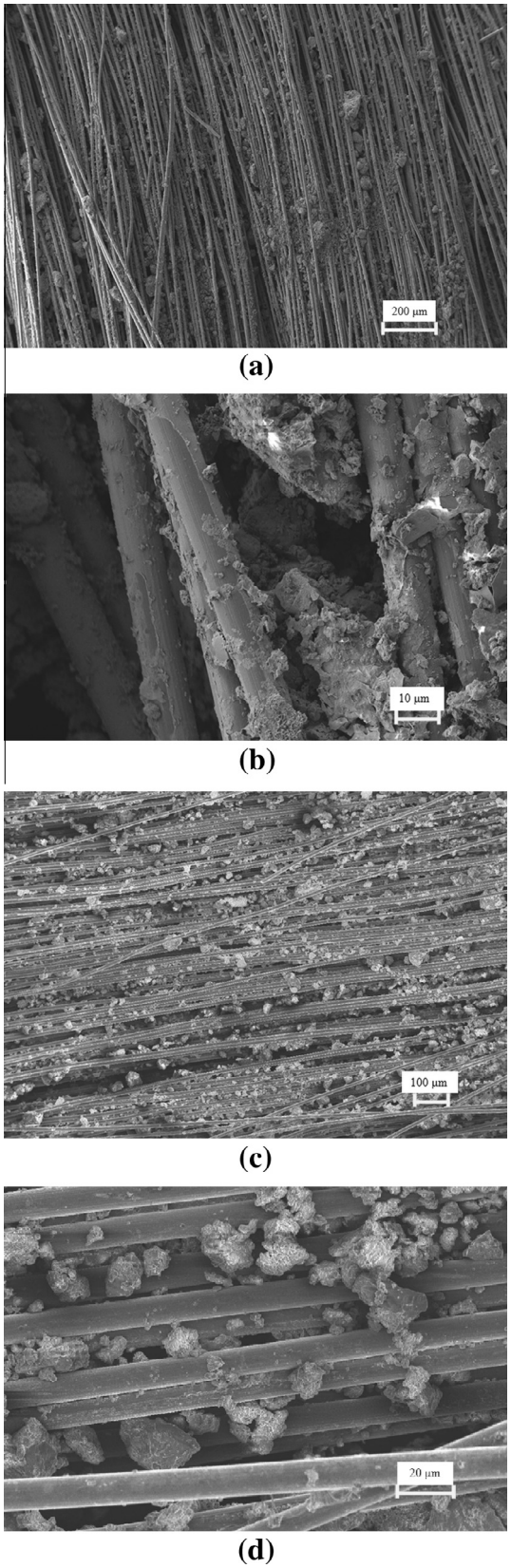

Fig. 2 – SEM photograph of the carbon fiber prepregs. (a) With pitch particles but without the organoclay at low magnification. (b) With pitch particles but without the organoclay at high magnification. (c) With pitch particles and the organoclay at low magnification. (d) With pitch particles and the organoclay at high magnification.

Section 2.2), clay particles in the amount of 4.00 g (unless stated otherwise) are hot-pressed in the absence of the pitch or the carbon fibers, using the same graphite mold and the same process as used for carbonization. Two types of clay particles are used, namely organoclay (Section 2.1) and sodium bentonite (without an organic component, Section 2.1), in order to investigate the effect of the organic component. Either type of clay is placed in the graphite mold under a nitrogen purge at a flow of 70 ml/min.

2.4. *Testing*

2.4.1. *Mechanical testing*

Longitudinal flexural testing of the unidirectional composites is conducted under three-point bending up to failure at a span of 20 mm, using a hydraulic mechanical testing system (MTS Systems Corp., Eden Prairie, MN). Two beam-shaped specimens are obtained from each 8-lamina composite disc by cutting along the diameter and along two parallel lines, so that each specimen has a width ranging from 9.1 to 10.3 mm, as separately measured for each specimen. Hence, two specimens are tested for each disc and at least 2 discs (separately fabricated) are tested for each composition. The flexural ductility is taken as the flexural strain at the maximum stress in the stress–strain curve up to failure. The flexural toughness, which corresponds to the work of fracture per unit volume, is the area under the stress–strain curve, with the area including the tail up to zero stress. The method of flexural testing is the same for the clays after hot pressing in the absence of the pitch or the carbon fibers to form a sheet.

2.4.2. *Thermal stability evaluation*

The thermal stability is evaluated under purging nitrogen by thermogravimetric analysis (TGA) using a thermogravimetric analyzer (TGA 7, Perkin–Elmer Corp.). In spite of the controlled nitrogen purge, air is present. The weight is measured at a heating rate of 5 °C/min from room temperature to 850 °C, immediately followed by furnace cooling at an approximate cooling rate of 15 °C/min.

2.4.3. *X-ray diffraction*

Powder XRD is conducted for the organoclay after hot pressing in the absence of the pitch or the carbon fibers. The material in the form of a sheet after the hot pressing has been ground into a powder by using a mortar and a pestle prior to XRD. The XRD involves CuKα radiation (40 kV, 30 mA) and a Siemens Kristalloflex D500 diffractometer equipped with a diffracted-beam graphite monochromator. The digital data collection is accomplished with Materials Data Inc. (Livermore, CA) Data Scan software.

2.4.4. *Raman scattering*

In order to characterize the carbon in the hot-pressed organoclay (without the pitch or the carbon fibers). Raman spectra are acquired using a Jobin–Yvon Horiba Labram HR spectrometer coupled to an Olympus BX41 microscope, using the 514.5 nm laser excitation from an Ar-ion laser. An 1800 lines/mm grating is used to acquire the spectra, yielding a spectral resolution greater than 2 cm^{-1}. The laser power

Table 1 – Thickness, true density and flexural properties of 8-lamina C/C composites with and without the filler.

	Without filler		With filler (without densification)
	Without densification	With densification	
Thickness (mm)	1.064 ± 0.003	1.012 ± 0.015	1.086 ± 0.006
True density (g/cm^3)	1.677 ± 0.001	1.692 ± 0.002	1.679 ± 0.008
Strength (MPa)	178.6 ± 3.6	235 ± 24	293.2 ± 24.3
Modulus (GPa)	37.6 ± 6.0	54.0 ± 0.4	55.0 ± 6.3
Ductility (%)	0.63 ± 0.32	0.49 ± 0.04	0.67 ± 0.15
Toughness (MJ/m^3)	2.0 ± 0.8	1.3 ± 0.1	2.9 ± 0.6

was kept below 1 mW to minimize local heating. The material is in a sheet form during Raman observation.

2.4.5. *Electrical resistivity measurement*

Measurement of the DC electrical resistivity is conducted for the clays after hot pressing in the absence of the pitch or the carbon fibers to form a sheet and is performed in the plane of the sheet, i.e., the plane perpendicular to the direction of hot pressing. As for flexural testing, each disc obtained by hot pressing is cut near the diameter of the disc to form two strips. The measurement is conducted by using a high-precision resistance multimeter (Keithley 2002) and silver paint (in conjunction with fine copper wires) for the electrical contacts. For the hot-pressed organoclay, the contacts are separated by a distance ranging from 3.2 to 3.9 mm, as separately measured for each specimen. For the hot-pressed sodium bentonite, the contacts are separated by a distance ranging from 2.1 to 3.1 mm, as separately measured for each specimen. The contacts cover the entirety of each of the two opposite large surfaces, with each surface containing the length and thickness of the strip. The length ranges from 18.2 to 28.3 mm for the hot-pressed organoclay and ranges from 23.5 to 26.4 mm for sodium bentonite, as separately measured for each specimen. The area of each contact is this length multiplied by the thickness of the disc. The thickness is 1.1 mm for the hot-pressed organoclay and ranges from 1.5 to 1.8 mm for sodium bentonite. The two-probe method is used, due to the high resistivity involved and the ineffectiveness of the four-probe method for this resistivity range.

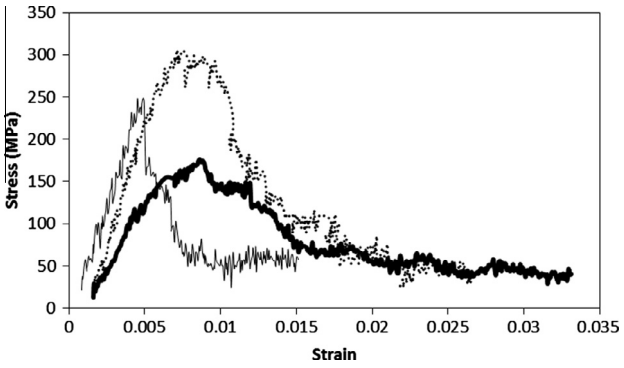

Fig. 3 – Representative flexural stress–strain curves of the C/C composites. Bold solid curve: composite without the filler or densification. Thin solid curve: composite without the filler but with densification. Dotted curve: composite with the filler but without densification.

2.4.6. *Density measurement*

The density of a material obtained after hot pressing is measured by weighing the specimen, calculation of the volume of the plate-shaped specimen based on the measured dimensions, and dividing the weight by the volume.

3. Results and discussion

3.1. *Prepreg morphology*

Scanning electron microscopy (SEM) shows the morphology of the carbon-fiber pitch-particle prepregs after drying but before pyrolysis (Fig. 2). Whether organoclay is present or not, the prepreg shows incomplete and inhomogeneous coverage of the fiber surface. The organoclay particles, which are much smaller than the pitch particles, mainly reside on the surface of the pitch particles. This is due to the fact that the pitch and organoclay particles are formed into a mixture prior to application to the fibers.

3.2. *Composite structure and properties*

The organic component in the organoclay cannot survive after the hot pressing. It is at least partly converted to carbon during the pyrolysis, as shown by Raman scattering (Section 3.3.1). Thus, after the hot pressing, the clay is referred to as a ceramic–carbon hybrid rather than organoclay.

The measured true density of the 8-lamina composite is increased by 0.9% by the densification and is essentially unaffected by the filler incorporation (without densification) (Table 1). The low fractional increase of the density upon densification is due to the high density prior to densification [12]. The density values are all around 1.68–1.69 g/cm^3 (Table 1), which is at the industrial target of 1.7 g/cm^3 [1], is higher than the value of 1.57 g/cm^3 previously reported for a C/C fabric composite containing a filler and fabricated by carbonization followed by densification [1], is close to the value of 1.67 g/cm^3 for a C/C composite containing carbon black [5], and is substantially higher than the value of 1.41 g/cm^3 previously reported for a C/C fabric composite without a filler and fabricated by carbonization followed by densification [1]. Based on the measured composite thickness, the fiber lamina thickness is 130–140 μm for all the composite of this work. The organoclay particles are believed to coat the exterior and parts of the interior of each tow.

The carbon yield of the mesophase pitch is estimated to be 80% [13]. The mass ratio of the fibers to the pitch to the organoclay of 50:40:10 thus corresponds to a mass ratio of the fibers to the carbon matrix to the organoclay of 50:32:10. With the loss on ignition being 43 wt.% for the organoclay (Section 2.1), 57% of the mass of the organoclay is assumed to remain as an inorganic solid (without organic component or carbon) after pyrolysis. This inorganic solid is a combination of disordered clay, mullite and cristobalite, as shown by XRD (Section 3.3.1), so this inorganic solid is in the form of ceramics. The carbon resulting from the carbonization of the organic component of the organoclay consists of ordered and disordered carbons in the graphite family (i.e., sp^2 carbons), as shown by Raman scattering (Section 3.3.1). The ceramics and carbon, both resulting from the organoclay, are in the form of a ceramic–carbon nanostructured hybrid, which is the filler present in the fabricated C/C composite. If the organic component of the organoclay has carbon yield of y by weight after carbonization, the mass ratio of the fibers to the carbon matrix to the hybrid filler becomes 50:32:(5.7 + 4.3 y). As shown in Section 3.4.2, y = 12%. Thus, the mass ratio of the fibers to the carbon matrix to the hybrid filler is 50:32:6.2, and the C/C composite with filler contains 56.7 wt.% fibers, 36.3 wt.% carbon matrix and 7.0 wt.% filler.

The measured true density ρ_o (1.677 g/cm^3, Table 1) of the composite without filler (without densification) is related to the true density of the carbon fibers (1.92 g/cm^3) and the density (ρ_m) of the carbon matrix (with the porosity included) according to the Rule of Mixtures, i.e.,

$$\rho_o = V_f(1.92) + (1 - V_f)\rho_m, \quad (1)$$

where V_f and $1 - V_f$ are the volume fractions of the fibers and the carbon matrix respectively. With the mass ratio of the fibers to the matrix being 50:32, i.e., fiber content = 61 wt.%, V_f is given by

$$V_f = (61/1.92)/[(61/1.92) + (39/\rho_m)]. \quad (2)$$

Substitution of Eq. (2) in Eq. (1) gives

$$\rho_m = 1.40 \text{ g/cm}^3. \quad (3)$$

Substitution of Eq. (3) in Eq. (2) gives V_f = 53 vol.%. This means that the matrix content is 47 vol.%.

If the carbon matrix in the absence of the porosity is assumed to be 1.8 g/cm^3 [14], the porosity in the carbon matrix (with the porosity included) is given by

$$\text{the porosity in the carbon matrix} = 1 - (1.41/1.8) = 22\%. \quad (4)$$

Although the calculation lumps the porosity with the carbon matrix, the porosity is not physically tied to the carbon matrix. The substantial porosity is a consequence of the low carbonization temperature of 1000 °C. This porosity is actually not only in the carbon matrix, which amounts to 47% of the volume of the overall composite, so the porosity of the overall composite is (0.47) (22%) = 10%. This porosity includes both open and closed pores. It is slightly higher than the open porosity of 8% for a C/C composite containing carbon black [5].

The true density ρ_o (1.692 g/cm^3, Table 1) of the composite without filler but with densification is related to the true density of the carbon fibers (1.92 g/cm^3) and the density (ρ_m) of the carbon matrix (with the porosity included) according to Eq. (1). Substitution of Eq. (2) in Eq. (1) gives

$$\rho_m = 1.43 \text{ g/cm}^3. \quad (5)$$

Substitution of Eq. (3) in Eq. (2) gives V_f = 54 vol.%. This means that the matrix content is 46 vol.%. The porosity in the carbon matrix (with the porosity included) is given by

$$\text{the porosity in the carbon matrix} = 1 - (1.43/1.8) = 21\%. \quad (6)$$

In the absence of a filler, the densification increases the matrix density from 1.40 to 1.43 g/cm^3, increases the fiber content from 53 to 54 vol.%, decreases the matrix content from 47 to 46 vol.%, and decreases the porosity in the matrix from 22% to 21%, and essentially does not affect the porosity (10%) in the overall composite.

The densification increases the flexural strength and modulus by 31% and 42% respectively (Table 1 and Fig. 3), as expected due to the increase in density. However, it decreases the flexural toughness and ductility by 38% and 22% respectively, probably due to the enhanced fiber–matrix bonding.

In the presence of the filler in the composite (without densification), the fibers, the matrix and the filler have mass ratio 56.7:36.3:7.0, and the true density ρ of the composite is given by

$$\rho = V_f(1.92) + V_m\rho_{m'} + V_h\rho_h, \quad (7)$$

where V_m and V_h are the volume fractions of the matrix and filler respectively, and $\rho_{m'}$ and ρ_h are the densities of the matrix and filler respectively. The density of the matrix ($\rho_{m'}$) is not the same as that for the composite without filler (ρ_m). With ρ = 1.679 g/cm^3 (Table 1), Eq. (7) gives

$$\rho_{m'} = 1.34 \text{ g/cm}^3. \quad (8)$$

Again assuming that the density of the carbon matrix without porosity is 1.8 g/cm^3,

$$\text{the porosity of the composite containing the filler} = 1 - (1.34/1.8) = 26\%. \quad (9)$$

This porosity is actually not only in the carbon matrix, which amounts to 45% of the volume of the overall composite, so the porosity of the overall composite is (0.45) (26%) = 12%. Hence, the composite with the filler incorporation (without

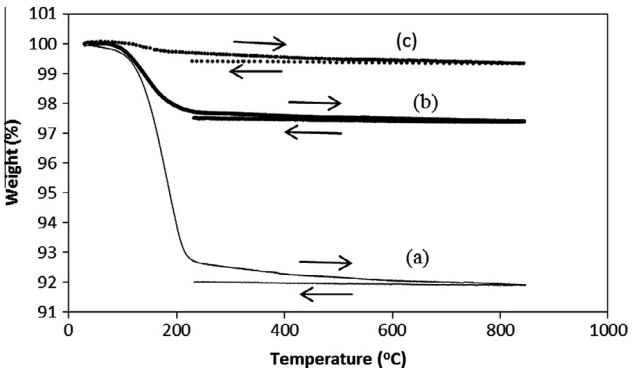

Fig. 4 – TGA curves of the C/C composites. (a) Composite without the filler or densification. (b) Composite without the filler but with densification. (c) Composite with the filler but without densification.

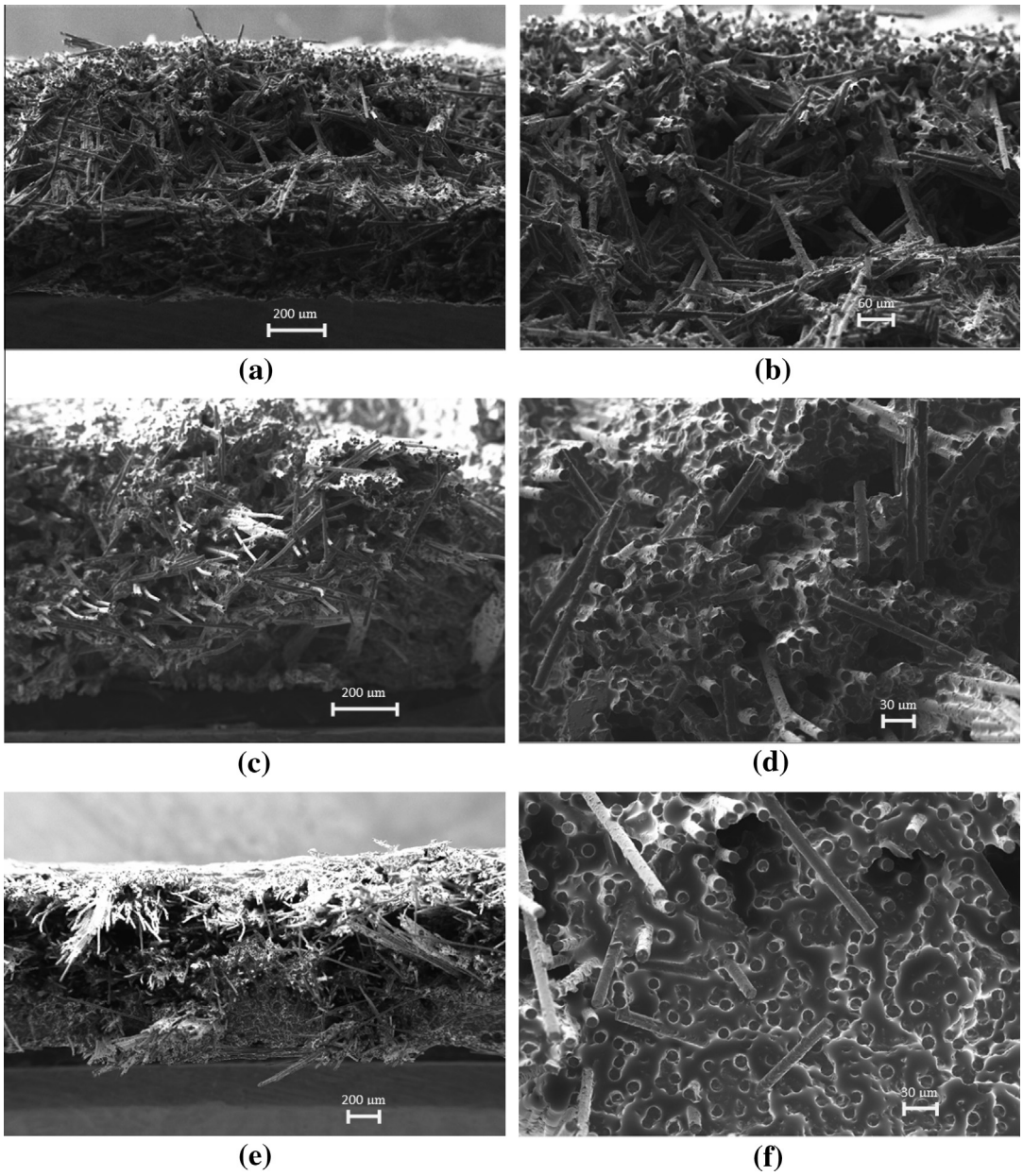

Fig. 5 – SEM photographs of the flexural fracture surfaces of the C/C composites. (a) and (b): Composite without the filler or densification. (c) and (d): Composite without the filler but with densification. (e) and (f): Composite with the filler but without densification.

densification) contains 57 wt.% (50 vol.%) fibers, 36 wt.% (33 vol.%) carbon matrix (with the porosity excluded), 7 wt.% (5 vol.%) filler, and 12% porosity.

The addition of the filler to the composite (without densification) causes the composite porosity to increase slightly from 10% to 12%, and causes the fiber volume fraction to decrease from 53% to 50%. In spite of the decrease in the fiber volume fraction and the slight increase in porosity, the filler addition (without densification) causes increases in the flexural strength (64% increase relative to the composite without the filler or densification), the flexural modulus (46% increase relative to the composite without the filler or densification) and the flexural toughness (45% increase relative to the composite without the filler or densification (Table 1 and Fig. 3). The ductility is essentially not affected by the filler addition. Relative to the composite without filler but with densification, the filler addition increases the flexural strength by 25%, increases the ductility by 37% and increases the toughness by 130%, with essentially no effect on the modulus. Thus, the properties of the composite with the filler but without densification are superior to those of the composite without the filler but with densification. It is practically significant that the incorporation of the filler produces a C/C composite that exhibits high flexural strength and modulus, in spite of the absence of densification.

The presence of mullite and cristobalite in the filler after hot pressing, as shown by XRD (Section 3.3.1), is believed to contribute to the effectiveness of the filler as a reinforcement.

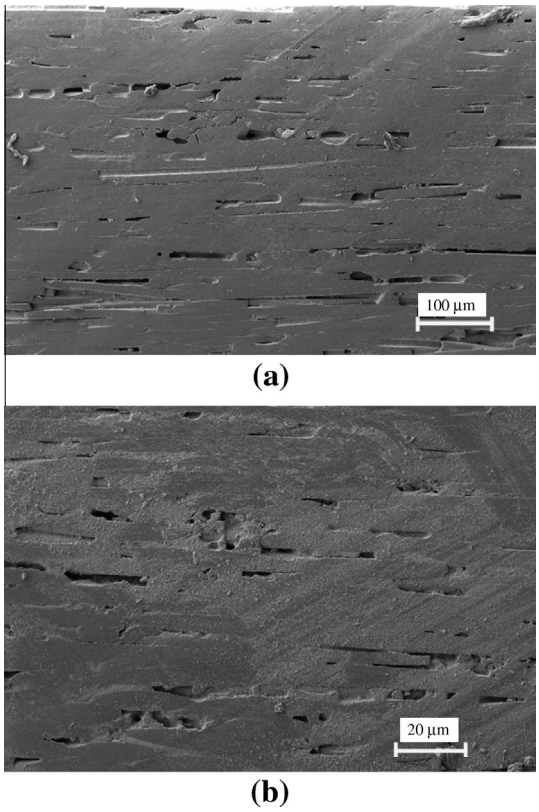

Fig. 6 – SEM photographs of the polished edge surface (surface perpendicular to the plane of the fibers) of the C/C composites. (a) Without the filler but with densification. (b) With the filler but without densification. The scale is not the same in (a) and (b).

Significant preferred orientation in the plane of the laminate is expected for the filler, due to the confined location of the filler between the carbon fiber laminae and the large aspect ratio of the filler. This preferred orientation probably also contributes to the effectiveness of the filler in increasing the flexural strength and modulus of the composite. However, an important cause for the ability of the filler to strengthen the C/C composite is that the filler is also a binder (Section 3.3). The improved binding enabled by the filler strengthens the composite.

Since the fibers are the dominant component for providing strength and modulus to the composite without the filler, the strength and modulus of this composite may be scaled (based on the Rule of Mixtures) to values corresponding to the fiber volume fraction in the composite containing the filler. This scaling allows study of the filler effect when the fiber volume fraction is fixed. With the scaling of the strength and modulus of the composite through multiplication by the factor 50/53 for the composite without densification and by the factor 50/54 for the composite with densification (i.e., when the fiber volume fraction is fixed at 50 vol.% for all the composites), the filler addition is thus found to increase the strength by 74% relative to the composite without the filler or densification and by 35% relative to the composite without the filler but with densification, and to increase the modulus by 55% relative to the composite without the filler or densification and

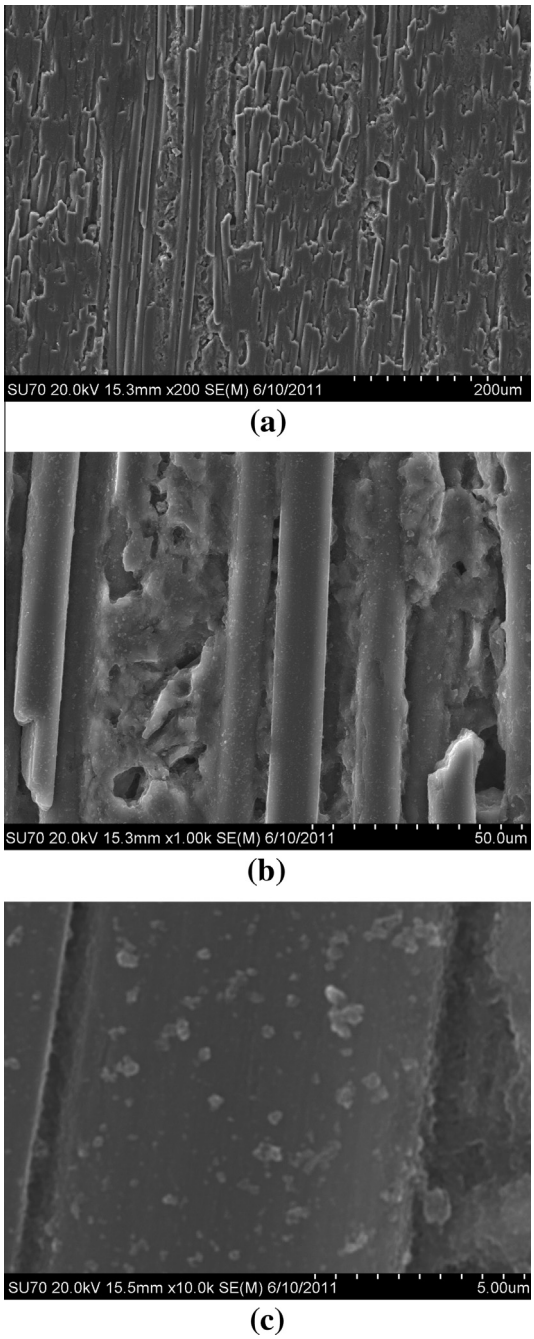

Fig. 7 – SEM photographs of the polished surface (surface in the plane of the fibers) of the C/C composite with the filler (without densification).

by 10% relative to the composite without the filler but with densification. The effect of the filler on the mechanical properties is more significant if the scaling is performed.

The flexural strength obtained in this work by filler incorporation (without densification) is 290 MPa, which is higher than the value of 120 MPa previously obtained by SiC incorporation (through liquid silicon infiltration) and pyrolysis at up to 900 °C without densification [4] and is much higher than the value of 42 MPa previously obtained by carbon black incorporation and pyrolysis at up to 2500 °C without densification [5]. It is also higher than the value of 179 MPa previously

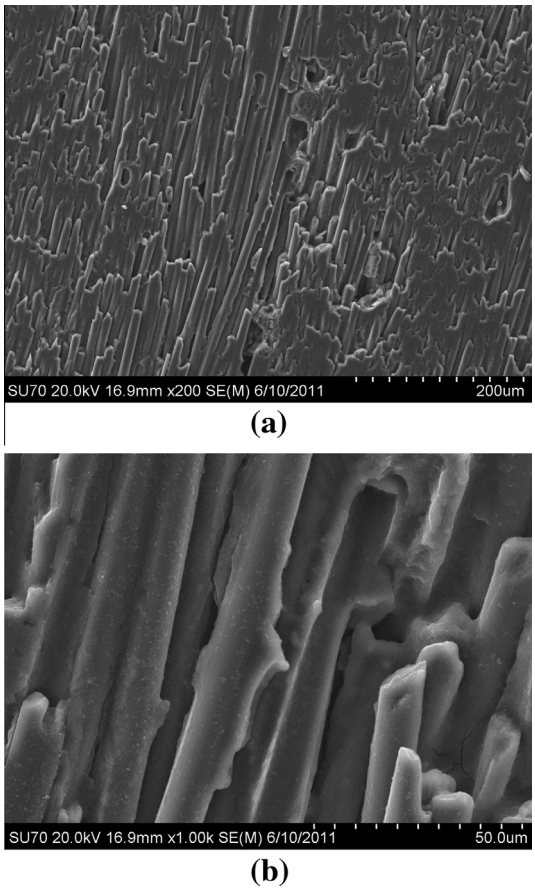

Fig. 8 – SEM photographs of the polished surface (surface in the plane of the fibers) of the C/C composite without the filler or densification.

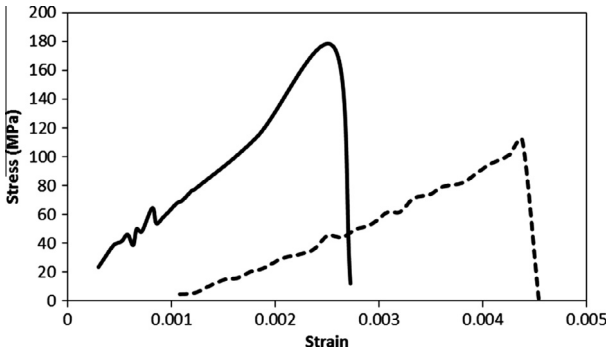

Fig. 9 – Representative flexural stress–strain curves for sheets obtained by hot pressing in the absence of the pitch or the fibers. Solid curve: the organoclay. Dashed curve: sodium bentonite.

reported for a C/C composite fabricated by CVI densification [6], and the value of 240 MPa for a C/C composite fabricated by wet impregnation and pulsating CVI [7].

The flexural modulus obtained in this work by filler incorporation is 55 GPa, which is higher than the value of 33 GPa for a C/C composite fabricated by CVI densification [6] and is much higher than the value of 7 GPa previously reported for a C/C composite [15], but is lower than the value of 87 GPa for a C/C composite fabricated by wet impregnation and pulsating CVI [16].

The high toughness of the C/C composite with filler is attributed to the large area of the interface between the ceramic and carbon components in the nanostructured hybrid filler and the nanoplatelet morphology of the filler. The slight slippage at the interfaces consumes mechanical energy during deformation.

The effect of the filler addition on the flexural strength is greater than that on the flexural modulus, whether the comparison is relative to the composite with or without densification. This means that the filler affects the fracture behavior more significantly than the elastic deformation behavior. This is consistent with the fact that the filler mainly resides at the interlaminar interface, which tends to be the site for damage to occur prior to fracture, and that the filler contributes to serving as a binder (Section 3.3).

For all the composites studied, the flexural fracture first occurs at the tension surface, followed by interlaminar fracture. This is in contrast to continuous carbon fiber epoxy-matrix

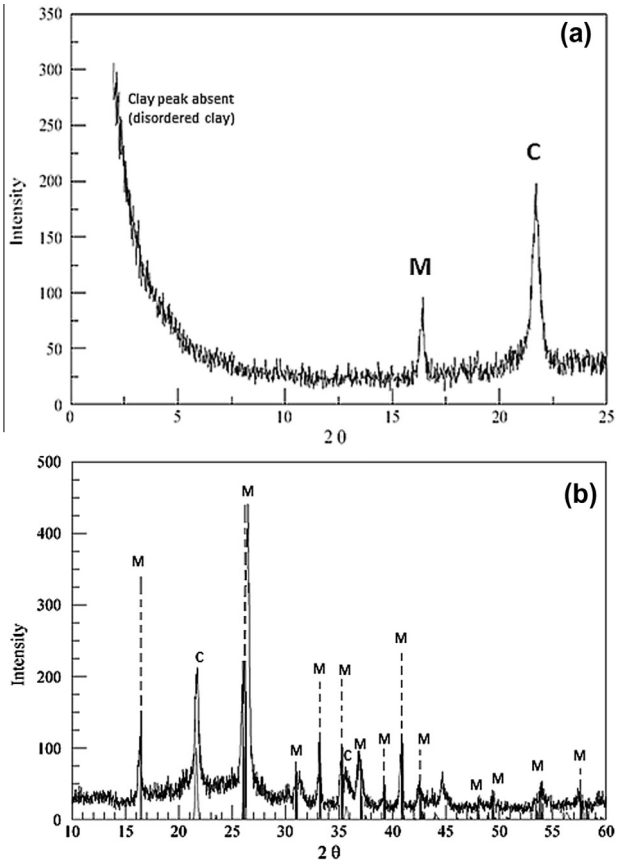

Fig. 10 – X-ray diffraction pattern of the material obtained by the hot pressing of the organoclay in the absence of the pitch or the fibers. M = mullite. C = cristobalite. (a) A low-angle XRD scan and (b) a higher-angle XRD scan. The dashed lines in (b) indicate the expected diffraction lines for mullite. The thin solid lines in (b) indicate the expected diffraction lines for cristobalite. No graphite peak is observed.

composites of prior work [17], for which flexural fracture first occurs at the compression surface. This behavior is attributed to the low ductility of carbon–matrix composites compared to polymer–matrix composites.

Fig. 4 shows TGA results for the composites. The thermal stability increases in the order: the composite without the filler and without densification, the composite without the filler but with densification, and the composite with the filler but without densification. The superior thermal stability of the composite with the filler but without densification compared to the composite without the filler but with densification is consistent with the superior flexural properties and with the previously reported improved oxidation resistance due to organoclay addition to a C/C composite [1]. Although the composite with the filler exhibits higher porosity (12%) than the composite without the filler (10%, whether with or without densification), the thermal stability is superior. This suggests that that the pores in the composite with the filler are less accessible than those in the composite without the filler, due to their smaller size, which is indicated by SEM observation (Fig. 6). However, further work is needed to distinguish between the accessible and inaccessible pores.

Fig. 5 shows the flexural fracture surfaces of the composites. With densification in the absence of the organoclay, the fibers become much better embedded in the carbon matrix and the extent of fiber pull-out [4,16,17] is reduced, as shown by comparing Fig. 5(a) and (b) with Fig. 5(c) and (d). This is consistent with the decreased toughness and the increased modulus and strength (Table 1). With the presence of the organoclay without densification, the matrix becomes more coherent than the composite without the organoclay but with densification, as shown by comparing Fig. 5(c) and (d) with

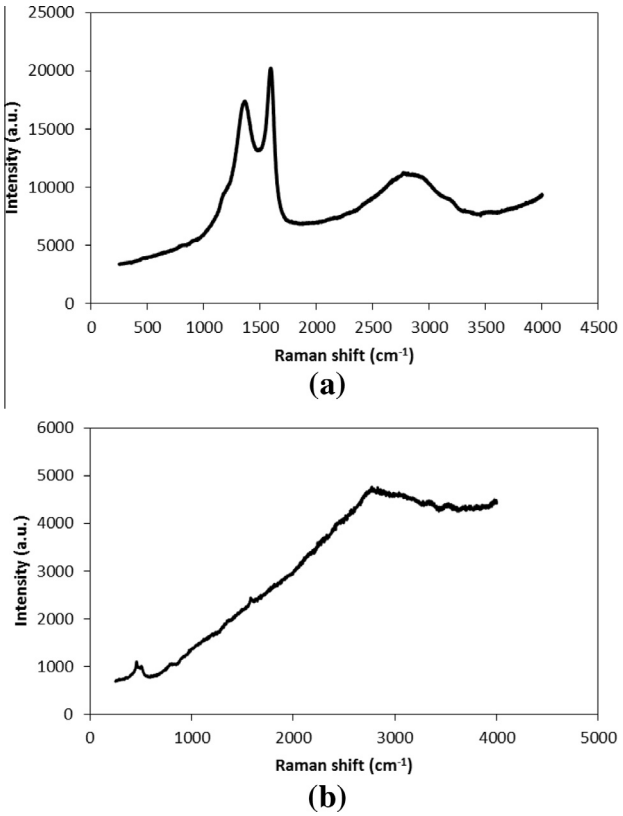

Fig. 11 – Raman spectra. (a) Hot-pressed organoclay, showing the disordered graphite peak at 1375 cm^{-1}, the ordered graphite peak at 1600 cm^{-1} and a broad peak at 2800 cm^{-1} (probably due to C–H). (b) Hot-pressed sodium bentonite, showing a weak peak at 470 cm^{-1} (probably due to Si–O–Si) and a weak broad peak at 2750 cm^{-1} (probably due to C–H).

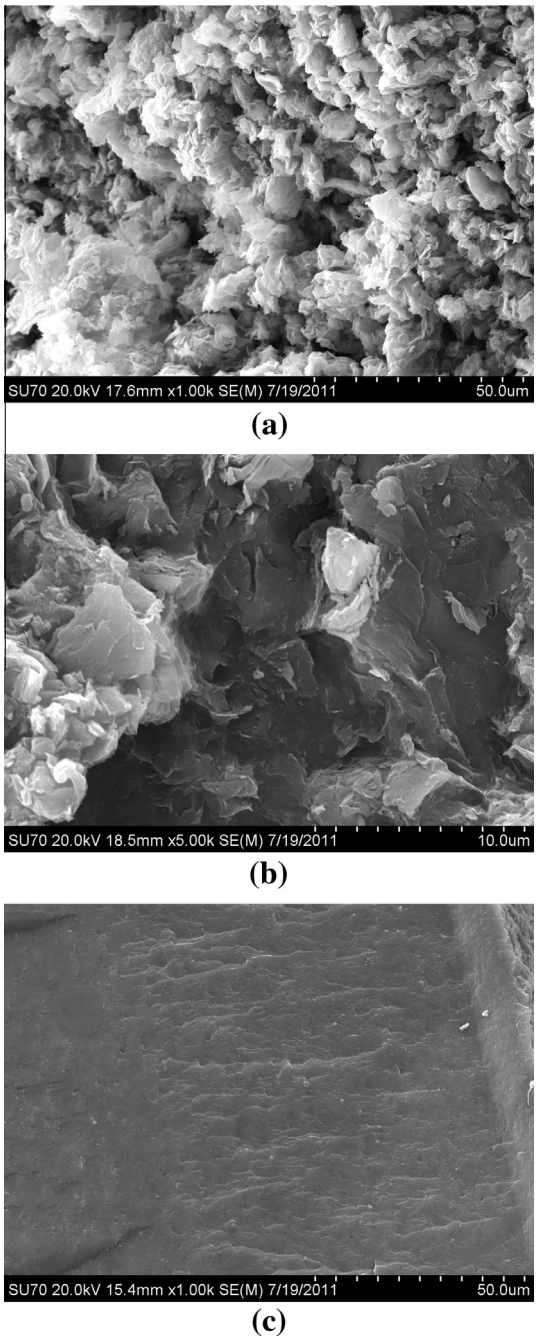

Fig. 12 – SEM photograph of hot-pressed organoclay, showing a continuous sheet and the absence of feathery particles. (a) Low magnification view of the plane of the sheet. (b) High magnification view of the plane of the sheet. (c) Fracture surface at the edge of the sheet, with the fracture obtained by bending the sheet.

Fig. 5(e) and (f). This is consistent with the increased strength (Table 1), while the increased toughness (Table 1) probably stems from the increased friction at the fiber–matrix interface. The increased friction probably relates to the refinement of the pore structure at the fiber–matrix interface.

Fig. 6 shows the SEM photographs of the polished edge surface (surface perpendicular to the plane of the fibers, with only one surface examined for each specimen) for the composite without the filler but with densification and for the composite with the filler but without densification. For both composites, pores that are elongated in the fiber direction are observed. The pores are on the average smaller in both length (in the fiber direction) and height (in the direction perpendicular to the plane of the fibers) for the composite with the filler than the composite without the filler. Based on visual observation, the average length is about 20 and 30 μm for the composites with and without the filler respectively. The average height is about 3 and 5 μm for the composites with and without the filler respectively. The pore dimensions reported here are approximate. Further work is needed to characterize the pore size.

Fig. 7 shows the SEM photographs of the polished surface (surface in the plane of the fibers) of the C/C composite containing the filler (without densification). The low-magnification photograph in Fig. 7(a) shows the absence of large pores. The higher-magnification photograph in Fig. 7(b) shows the matrix surrounding the fibers, with the filler not observable inside the matrix. However, at an even higher magnification (Fig. 7(c)), flakes that are mainly submicron in lateral size and that resemble filler platelets are observed on the surface of the fibers.

Fig. 8 shows the polished surface of the C/C composite without the filler or densification. The degree of coverage of the fibers by the carbon matrix is lower than those for the composite with the filler.

Although the porosity is slightly higher in the composite with the filler, the pore size is likely smaller in the presence of the filler, as suggested by comparing Figs. 7 and 8. Large pores are highly detrimental to the mechanical properties of C/C composites [16]. It was reported that, despite the increase in the true density of the composite, the flexural strength does not increase, due to the presence of large pores [16]. The ability of filler incorporation to increase the flexural strength is believed to be partly due to the decrease in the pore size.

It was previously reported that the porosity of a C/C fabric composite is decreased by the incorporation of SiC nanoparticles, but the porosity reported was macroscopic porosity that was observed at a low magnification (25×) [1]. Pores of size 50 μm were previously observed at a higher magnification (1000×) in C/C composites even after multiple cycles of impregnation and re-carbonization [16]. In contrast, the porosity reported here includes pores of all sizes. The high macroscopic porosity previously reported for the composite without a filler partly stems from the fabric nature of the carbon fibers used [1]. In contrast, this work uses non-woven carbon fiber tows. Comparison of the microscope photographs of this work and those of Ref. [1] suggests that the macroporosity is considerably lower for the composites of this work than those of Ref. [1].

It was previously reported that filler incorporation increases the true density of a C/C composite slightly [1]. In contrast, this work observes no change in the true density upon filler incorporation (case without densification). This difference is at least partly due to the occurrence of densification in prior work [1] and the absence of densification in this work for the composite with the filler. The microscopic pores generated in the composite after carbonization by the presence of the filler may be filled to a degree during densification.

It was previously reported that the open porosity of a C/C composite is decreased from 9% to 8% by carbon black incorporation [5]. This effect of carbon black relates to the porous aggregate structure of carbon black and the consequent high compressibility (squishability) of carbon black. The squishability results in conformability as the carbon black is compressed, thus enabling carbon black to fill small spaces, thereby reducing the porosity. In contrast, the filler is not squishable.

It was previously reported that CNT growth on carbon fibers increases the true density of a C/C composite [6]. The CNT is not squishable, but its small diameter enables it to fit into small spaces, thereby enhancing its ability to reduce the porosity.

3.3. *Clays hot-pressed in the absence of the pitch or the carbon fibers*

3.3.1. *Hot-pressed organoclay*

The yield of the organoclay after hot pressing is (49.8 ± 0.3)% by mass, as obtained by weighing before and after the hot pressing. The weight loss [(50.2 ± 0.3)%] due to the hot pressing is contributed by both the ceramic and organic components of the organoclay, as shown by the fact that the loss on ignition is 43 wt.% (according to the organoclay manufacturer).

Before hot pressing, the organoclay is in the form of particles. After hot pressing the organoclay (4.00 g) in the absence of the pitch or the carbon fibers, the organoclay becomes a coherent sheet of thickness 1.1 mm and true density 2.366 g/cm^3. This means that the organoclay has binding ability, which contributes to the effectiveness of the filler in reinforcing the C/C composites (Section 3.2).

Flexural testing of strips cut from the sheet formed by hot pressing 4.00 g of organoclay gives strength 175.5 ± 3.2 MPa, modulus 69.4 ± 2.5 GPa, toughness 0.23 ± 0.02 MPa and ductility (0.26 ± 0.01)%. A representative flexural stress–strain curve is shown in Fig. 9. The tail present in each of the stress–strain curves for the C/C composites at strains above that at the highest stress (Fig. 3) is absent in Fig. 9. Comparison of the flexural property values of the hot-pressed organoclay with those in Table 1 for the C/C composites shows that (i) the flexural strength of the hot-pressed organoclay is similar to that of the C/C composite without the filler or densification, but is lower than that of the C/C composite without the filler but with densification and lower than that of the C/C composite with the filler, (ii) the flexural modulus is higher than all of the values in Table 1, (iii) the flexural ductility is lower than all of the values in Table 1, and (iv) the flexural toughness is much lower than all of the values in Table 1. The low ductility, low toughness and the absence of a tail in the stress–strain

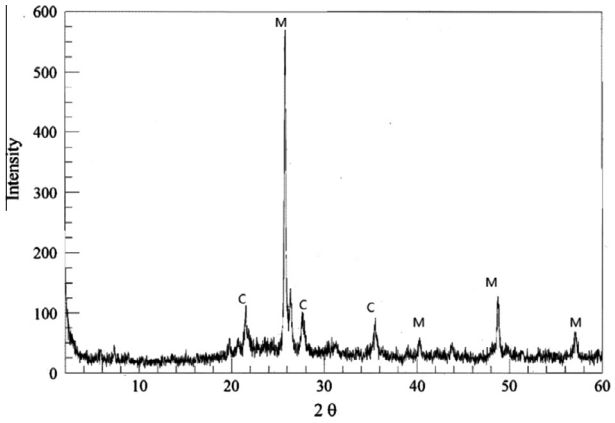

Fig. 13 – X-ray diffraction pattern of the material obtained by the hot pressing of sodium bentonite in the absence of the pitch or the fibers. M = mullite. C = cristobalite.

curve are consistent with the absence of fibers. The high modulus and strength of the hot-pressed organoclay are consistent with the effectiveness of the filler in reinforcing the C/C composites (Section 3.2).

The modulus of hot-pressed organoclay (69 GPa) is much higher than that of graphite (in the range from 11 to 12 GPa [18]) and is equal to that of soda-lime glass (69 GPa [18]), though it is lower than that of 90% pure alumina (275 GPa [18]). The flexural strength of hot-pressed organoclay (176 MPa) is much higher than the tensile strength of graphite (in the range from 31 to 69 MPa [18]) and is much higher than the tensile strength of soda-lime glass (69 MPa [18]), though it is lower than the tensile strength of 90% pure alumina (337 MPa [18]).

Powder XRD conducted for organoclay prior to hot pressing (Fig. 1(a)) shows that the organoclay is mainly montmorillonite with basal spacing d_{001} = 31.5 Å, which is consistent with the value provided by the manufacturer of the organoclay. For the material obtained by the hot pressing of organoclay in the absence of pitch, Fig. 10(a) shows that the montmorillonite is disordered and Fig. 10(b) shows that mullite and cristobalite (SiO_2, without distinction between the α and β forms of cristobalite) have formed. Mullite contains about 60 mol% Al_2O_3 and is a phase in the SiO_2–Al_2O_3 binary phase diagram. The transformation of kaolinite to mullite upon heating to 1150 °C has been previously reported [19,20]. The transformation of kaolinite to mullite and cristobalite upon similar heating has also been reported [19]. Both mullite and cristobalite are attractive for their high stiffness, high hardness and high melting temperatures (1890 and 1713 °C for mullite and cristobalite respectively). In addition, the hot pressing causes the clay to lose water (both interlayer water molecules and structural hydroxyls) and become disordered, as shown by the disappearance of the organoclay peak (31.5 Å, Fig. 1(a)) and the appearance of a long tail that rises at low diffraction angles. In other words, the inorganic component in the organoclay has become a multi-phase mixture of mullite, cristobalite and disordered clay. No graphite diffraction peak is observed in the organoclay after hot pressing, possibly due to the turbostratic nature of the carbon.

Raman scattering shows that the hot pressing of the organoclay results in the formation of carbon. Both the 1600 cm^{-1} E_{2g2} graphite peak and the 1375 cm^{-1} disordered graphite peak are observed [21] (Fig. 11(a)), indicating the presence of solid carbon in the graphite family. A broad and relatively weak peak centered at 2800 cm^{-1} is also observed and is probably due to the C–H stretch vibration.[3] Moreover, the organoclay after hot pressing is black, whereas that before hot pressing is white. The electrical resistivity is $(6.40 \pm 0.84) \times 10^6$ Ω cm for the organoclay after hot pressing.

The phases in the hot-pressed organoclay include mullite, cristobalite, disordered clay, ordered carbon and disordered carbon. The ordered and disordered carbons, both in the graphite family, are formed by the carbonization of the organic component of organoclay. Hot-pressed organoclay is a new ceramic–carbon hybrid nanomaterial.

The hybrid formed by hot pressing organoclay in the absence of the pitch or the carbon fibers is a continuous sheet of size limited by the size of the mold cavity (diameter 31.8 mm in this work). The surface morphology of the sheet (Fig. 12(a) and (b)) has essentially no remnant of the feathery structure of the particles prior to hot pressing (Fig. 1(b)). The fracture surface at the edge of the sheet, as obtained by bending the sheet, shows roughly parallel striations (Fig. 12(c)) that suggest a degree of preferred orientation in the sheet. Preferred orientation is expected due to the layered structure of clay and the presence of pressure in the direction perpendicular to the plane of the sheet during the hot pressing.

TGA shows a weight loss of 0.02% upon heating to 850 °C, compared to a corresponding value of 0.6% for the C/C composite with the organoclay (Fig. 4). This means that the hot-pressed organoclay is much more oxidation resistant than the C/C composite with the organoclay. The superior thermal stability of hot-pressed organoclay is partly attributed to the relatively low porosity, as suggested by the absence of pores in the fracture surface micrograph in Fig. 12(c) and the presence of pores (black regions) in the fracture surface micrograph in Fig. 5(f) for the C/C composite with the organoclay. It is also partly attributed to the relatively low carbon content (14 vol.%, Section 3.4.2) of the hot-pressed organoclay and the superior high-temperature stability of the ceramic component (86 vol.%, Section 3.4.2) compared to the carbon component of the hot-pressed organoclay.

The ceramic–carbon hybrid of this work is nanoscale and layered in structure, due to such a structure in the organoclay. In contrast, ceramic–carbon hybrids of prior work do not exhibit such as structure and are obtained by using methods that are different from that of this work, as described below. A hybrid of pitch-based carbon (40 wt.%) and montmorillonite (not organoclay), as obtained by heating at 1200 °C in a nitrogen purge (without pressure application) pitch together with a honeycomb-shaped molded montmorillonite monolith (molded by mixing with water, followed by drying), exhibits electrical resistivity 9×10^{-2} Ω cm and unreported mechanical properties; the resulting hybrid does not exhibit a layered

[3] http://www.horiba.com/fileadmin/uploads/Scientific/Documents/Raman/bands.pdf.

Table 2 – Weight loss at various temperatures during heating under identical conditions.

Material (hot-pressed)		200 °C (%)	400 °C (%)	600 °C (%)	800 °C (%)
Without carbon fibers or pitch	Organoclay	0.014	0.042	0.063	0.084
	Sodium bentonite	0.016	0.098	0.015	0.187
With carbon fibers and pitch	C/C without densification	6.096	7.730	7.945	8.052
	C/C with densification	2.100	2.430	2.514	2.590
	C/C with organoclay but without densification	0.344	0.527	0.618	0.699

structure or a nanostructure; the low resistivity is consistent with the high carbon content [22]. A hybrid of kaolinite clay (not organoclay) and crystalline graphite is obtained by heating at 1,100 °C for 2 h in a reducing atmosphere a compact of a mixture of the clay and graphite powders, both of particle size 50 μm; the resulting material does not exhibit a layered structure, but a particulate structure, with the phases including crystalline graphite, cristobalite and disordered clay, and with unreported mechanical properties [23]. Carbon present in a hybrid and corresponding to either pitch-based carbon [22] or the crystalline graphite used as an ingredient [23] differs in crystallographic order, microstructural feature size and/or geometry from carbon resulting from the carbonization of the nanoscale organic layers of organoclay in this work.

In another prior work, SiC and carbon are formed as the matrix of a composite by the co-deposition of propane (a carbon precursor) and methyltrichlorosilane (a silicon carbide precursor) [24,25]. The resulting SiC–C hybrid does not exhibit a layered structure, but is in the form of a random mixture of the two phases. In yet another prior work, the addition of SiC particles to a C/C composite gives a hybrid that involves SiC particles in a carbon matrix [26]. Still other prior work involved a zeolite–carbon hybrid obtained by calcination and carbonization followed by a hydrothermal treatment; the resulting material exhibits a structure that is dominated by pores [27,28]. In addition, a hybrid of zeolite and activated carbon prepared from elutrilithe and pitch by pyrolysis, activation and then hydrothermal treatment is also dominated by pores [29].

The C/C composites of Section 3.2 are strengthened by the new hybrid that is formed from organoclay during the pyrolysis of the C/C composites. The hybrid serves as a filler as well as a binder. The process can be called co-carbonization, as the carbonization of the pitch to form the carbon matrix of the C/C composite and the carbonization of the organic component of the organoclay to form the carbon in the hybrid occur at the same time.

3.3.2. *Hot-pressed sodium bentonite*

The yield of the sodium bentonite after hot pressing is (79 ± 3)% by mass. That the yield is not 100% means that there are volatile components evolved during the decomposition of the clay. This is consistent with the fact that the weight loss in connection with the yield of the organoclay exceeds that of the loss on ignition (Section 3.3.1).

The sodium bentonite is light grey in color before hot pressing and is dark grey (but not black) after hot pressing. XRD of the hot-pressed sodium bentonite shows mullite, cristobalite and disordered clay (Fig. 13), as for the hot-pressed organoclay, although the number of peaks is smaller than that for the hot-pressed organoclay (Fig. 10(b)). This means that the presence of the organic component influences the formation of the ceramic phases from the inorganic component. The Raman spectrum of hot-pressed sodium bentonite (Fig. 11(b)) shows no peak other than a broad weak peak centered around 2750 cm^{-1} that may be due to the C–H stretch vibration and a very weak peak at 470 cm^{-1} that may be due to the Si–O–Si vibration.[4] Thus, solid carbon is not formed by hot-pressing sodium bentonite, as expected.

The hot pressing of sodium bentonite yields a coherent sheet, as for the hot pressing of the organoclay. The electrical resistivity after hot pressing, as measured on sheets, with each sheet being made from sodium bentonite of mass ranging from 4.00 to 8.00 g and of thickness ranging from 1.5 to 3.3 mm (as separately measured for each specimen), is $(1.63 \pm 0.12) \times 10^7\ \Omega$ cm, which is higher than the value of $(6.40 \pm 0.84) \times 10^6\ \Omega$ cm for the hot-pressed organoclay. The true density is 2.470 g/cm^3. Flexural testing of the hot-pressed sodium bentonite (sheet of thickness 2.11 ± 0.04 mm and true density 2.47 g/cm^3 and made by hot pressing 6.00 g of sodium bentonite) gives strength 107.4 ± 5.0 MPa (lower than the value of 175 MPa for the hot-pressed organoclay), modulus 31.2 ± 0.2 GPa (much lower than the value of 69 GPa for the hot-pressed organoclay), ductility (0.40 ± 0.04)% (higher than the value of 0.26% for hot-pressed organoclay), and toughness (0.175 ± 0.002) MPa (lower than the value of 0.23 MPa for hot-pressed organoclay). A representative stress–strain curve of hot-pressed sodium bentonite is shown in Fig. 9. The curve shows no tail, as in the case of the hot-pressed organoclay (Fig. 9).

Based on the relatively poor mechanical properties, sodium bentonite is not as good a binder as organoclay, as expected from the fact that sodium bentonite does not contain an organic component. Based on the color, the electrical resistivity and the Raman results of the hot-pressed material and the absence of an organic component prior to hot pressing, the hot-pressed sodium bentonite does not contain carbon. The absence of carbon in hot-pressed sodium bentonite contributes to causing the low strength, low modulus and high ductility compared to hot-pressed organoclay. Neverthe-

[4] http://www.horiba.com/fileadmin/uploads/Scientific/Documents/Raman/bands.pdf.

less, even though an organic component is absent, sodium bentonite has some binding ability.

The modulus of hot-pressed organoclay (31 GPa) is much higher than that of graphite (in the range from 11 to 12 GPa [18]), but is lower than that of soda-lime glass (69 GPa [18]) and that of 90% pure alumina (275 GPa [18]). The flexural strength of hot-pressed organoclay (107 MPa) is much higher than the tensile strength of graphite (in the range from 31 to 69 MPa [18]) and is much higher than the tensile strength of soda-lime glass (69 MPa [18]), though it is lower than the tensile strength of 90% pure alumina (337 MPa [18]).

3.4. *Thermal stability and further structural analysis*

3.4.1. *Thermal stability*

Table 2 shows that the thermal stability is superior for hot-pressed organoclay than hot-pressed sodium bentonite. This is consistent with the superior binding ability of organoclay and the possible consequence of less porosity. Table 2 also shows that both the hot-pressed organoclay and the hot-pressed sodium bentonite are much superior to any of the three types of C/C composite in the thermal stability, as expected from the relatively low porosity and the relatively low proportion of carbon in the materials without the carbon fibers. The weight loss of hot-pressed organoclay at 800 °C is 0.08%, compared to 0.7% for the C/C composite with the organoclay.

3.4.2. *Structure of the ceramic–carbon hybrid*

The organoclay has 57 wt.% ceramic component and 43 wt.% organic component. Since the yield of the sodium bentonite is 79%, the yield of the ceramic component of the organoclay after hot pressing is taken as 79%. The yield of the organoclay (both ceramic and organic components considered together) is 50%. This means that the yield of the organic component of the organoclay is 12%.

Since (i) the organoclay before hot pressing has 57 wt.% ceramic component and 43 wt.% organic component, (ii) the ceramic component has a yield of 79% after hot pressing, and (iii) the yield of the organic component is 12%, the mass ratio of the ceramic component to the carbon component after hot pressing is 57(0.79):43(0.12), i.e., 45:5.2. In other words, the hybrid contains 89.7 wt.% ceramic component and 10.3 wt.% carbon component.

Based on the true density of the ceramic–carbon hybrid (i.e., the hot-pressed organoclay, 2.366 g/cm^3, Section 3.3.1) and the true density of the ceramic part of the hybrid (i.e., the hot-pressed sodium bentonite, 2.470 g/cm^3, Section 3.3.2), the proportion of the constituents of the hybrid can be calculated by using the Rule of Mixtures for the true density.

$$2.366 = 2.470\ V_c + \rho_{hc}(1 - V_c), \tag{10}$$

where V_c is the volume fraction of the ceramic component in the hybrid, $(1 - V_c)$ is the volume fraction of the carbon component in the hybrid, and ρ_{hc} is the density of the carbon in the hybrid. Based on the abovementioned fact that the hybrid contains 89.7 wt.% ceramic component and 10.3 wt.% carbon component,

$$1 - V_c = (10.3/\rho_{hc})/[(89.7/2.470) + (10.3/\rho_{hc})]. \tag{11}$$

Simultaneous solution of Eq. (10) and (11) gives $V_c = 0.86$ and $\rho_{hc} = 1.73$ g/cm^3. Hence, the ceramic component of the hybrid amounts to 86 vol.% whereas the carbon component of the hybrid amounts to 14 vol.%. The density 1.73 g/cm^3 of the carbon component is higher than the density $\rho_{m'} = 1.34$ g/cm^3 of the carbon matrix in the C/C composite containing the filler (Section 3.2). Assuming that the true density is 1.8 g/cm^3 [14] for carbon without porosity, the porosity in the carbon component of the hybrid is 4%.

The ceramic component of the hybrid consists of mullite, cristobalite and disordered clay. Based on the relative intensities of the XRD peaks in Fig. 9(a), it is estimated that the volume fraction of mullite is twice of that of cristobalite. Based on the Rule of Mixtures for the true density of the ceramic component,

$$2.470 = 3.16\ V_u + 2.33\ V_u/2 + 2.457(1 - 1.5\ V_u), \tag{12}$$

where 3.16, 2.33 and 2.457 g/cm^3 are the densities of mullite, cristobalite and clay (bentonite [30]) respectively. Solution of Eq. (12) gives $V_u = 0.02$. This means that the ceramic component of the hybrid contains 2 vol.% mullite, 1 vol.% cristobalite and 97 vol.% disordered clay. If the volume fraction of mullite is equal to that of cristobalite, a similar calculation gives similar results, namely 2 vol.% mullite, 2 vol.% cristobalite and 96 vol.% disordered clay. Thus, the result is not very sensitive to the ratio of mullite to cristobalite.

3.4.3. *Structure of the C/C composite containing the ceramic–carbon hybrid*

The true density of the hybrid (2.366 g/cm^3, Section 3.3.1) allows the conversion of the proportions of the fibers, the carbon matrix and the hybrid filler from mass fractions to volume fractions. The mass fractions are 56.5 wt.% fibers, 36.2 wt.% carbon matrix and 7.3 wt.% hybrid (Section 3.2). Hence, the C/C composite contains 50 vol.% fibers, 45 vol.% carbon matrix (or 33 vol.% carbon matrix without porosity plus 12% porosity) and 5 vol.% hybrid. If the carbon in the hybrid filler and the carbon in the matrix (derived from the pitch) are considered together, the total carbon content would amount to 46 vol.%, while the ceramic part of the hybrid filler would amount to 4 vol.% of the overall composite.

3.5. *Scientific and technological significance*

Hot-pressed organoclay is a new ceramic–carbon hybrid nanostructured material. The C/C composites are strengthened by this hybrid that is formed from the organoclay during pyrolysis. The organoclay and the pitch (an additional binder) are pyrolyzed at the same time. The hybrid serves both as a filler and a binder. Both the organic and inorganic components of the organoclay contribute to serving as a binder. The combination of the filler and binder functions in the same ingredient is a new concept. That the hybrid serves both functions almost guarantees good bonding between the filler and the carbon that coexist in the hybrid and furthermore guarantees that the hybrid is nanostructured (since the ceramic and carbon are formed simultaneously *in situ* from the organoclay, which is nanostructured). The fact the hybrid

serves as a binder also reduces the need for an additional carbon matrix precursor (such as pitch).

The ceramic–carbon hybrid has the ceramic part being the vast majority and the carbon part being the minority. This means that the resulting C/C composite contains a substantial proportion of ceramic phases, which are attractive for their high temperature ability. In other words, the hybrid also serves to enhance the oxidation resistance of the resulting C/C composite. This method of introduction of ceramics to a C/C composite differs from the conventional method that involves coating a C/C composite with a ceramic material such as silicon carbide. The coating process adds to the cost and the difference in thermal expansion coefficient between the coating and the C/C composite underneath can cause debonding of the coating during service.

The incorporation of the ceramic–carbon hybrid in a C/C composite improves the mechanical properties and oxidation resistance, such that the densification step that typically follows pyrolysis in the fabrication of a C/C composite may be eliminated. This elimination means much cost saving, thereby widening the applications of C/C composites.

Both the processing cost and the material cost are much lower for the ceramic–carbon hybrid monolith than those of C/C composites, because the processing simply involves hot-pressing a single type of powder, without subsequent densification. Both the hybrid and the hot-pressed sodium bentonite exhibit strength and modulus that are much higher than those of graphite.

3.6. *Possible extension of the concept of this work*

The precursor material of the ceramic–carbon hybrid can be organoclay in a nanotube form [31], although this work uses organoclay in a layered particulate form. Organoclay, even that in the nanotube form, is inexpensive, because clay is a natural mineral. Moreover, organoclay can involve a large variety of organic materials, including those that are excellent carbon matrix precursors (such as polyacrylonitrile, or PAN). The layered (smectite) form of organoclay, as used in this work, allows a large interface area between the ceramic and carbon nanoscale layers in the resulting ceramic–carbon hybrid, thereby enabling the ceramic structure to protect the carbon from oxidation. On the other hand, the nanotube form of organoclay is expected to allow the carbon residing in the axial channel of the resulting ceramic–carbon hybrid nanotube to resemble a carbon nanofiber of diameter of the order of 10s of Angstroms. The carbon nanofiber form is expected to be advantageous for reinforcing the resulting C/C composite. Moreover, depending on the type of clay in the organoclay, the ceramic phase that is formed *in situ* from the organoclay during pyrolysis may differ, thus possibly allowing the tailoring of the ceramic phase by the choice of the type of clay.

It is expected that the binding ability and the reinforcing ability of the ceramic–carbon hybrid can be controlled by (i) the choice of the clay part (in terms of both the composition and the morphology) of the organoclay, (ii) the choice of the organic part (in terms of the molecular structure, the carbon yield and the degree of order in the resulting carbon, and the degree of graphitization in case that graphitization is conducted after the carbonization) of the organoclay, and (iii) the choice of the proportions of the clay and organic parts of the organoclay. The proportion of organoclay used along with the carbon fibers and conventional carbon matrix precursor is another variable in the material design. There is much room for further development of the technology presented in this paper.

Although this paper uses organoclay to form the ceramic–carbon hybrid, other forms of organo-modified minerals [32–34] may be used instead of organoclay. In general, the choice of the inorganic component of an organo-modified mineral would govern the composition of the ceramic component of the resulting ceramic–carbon hybrid. It is possible for the organic component to affect the composition of the ceramic component of the resulting ceramic–carbon hybrid.

In this paper, the function of the ceramic part of the ceramic–carbon hybrid is reinforcement. However, in general, the ceramic component may be designed for other functions, such as those related to electrical and thermal applications.

This work reports for the first time (i) the feasibility of conversion of the organic component of organoclay to carbon and the associated feasibility of forming a ceramic–carbon hybrid by pyrolysis, (ii) the feasibility of forming a monolithic material from organoclay by pyrolysis when it is alone, in the absence of any other ingredient, (iii) the mechanical properties, thermal stability and microstructure of the hybrid, (iv) the feasibility of organoclay serving as both reinforcing filler and binder at the same time, and (v) the feasibility of using organoclay incorporation to facilitate the low-cost fabrication of C/C composites without densification, such that the resulting composites exhibit superior mechanical properties and thermal stability than composites without the hybrid.

4. Conclusion

A new ceramic–carbon nanostructured hybrid (86 vol.% ceramics, 14 vol.% carbon) formed from montmorillonite-based organoclay during pyrolysis is reported. The clay has been intercalated with a quaternary ammonium salt (dimethyl, dihydrogenated tallow) with chloride anions. The ceramic component of the ceramic–carbon hybrid functions as a reinforcing filler, while its carbon component serves as a matrix for C/C composites. The carbon yield of the organic component of the organoclay is 12%. In the hybrid, the ceramic component is a multi-phase material comprising disordered clay (~97 vol.% of the ceramic component), mullite (~2 vol.% of the ceramic component) and cristobalite (~1 vol.% of the ceramic component), and the carbon component comprises disordered carbon and ordered carbon in the graphite family. During pyrolysis, the ordered organoclay (d_{001} 31.5 Å) is transformed to mullite, cristobalite and disordered clay, allowing the clay part of the organoclay to serve as both binder and reinforcement. The organic part serves as a binder.

In the fabrication of the C/C composite, carbon fiber tows are immersed in an aqueous dispersion of a mixture of the organoclay and the pitch powder (20 μm size) to form prepreg sheets, which are unidirectionally stacked and carbonized at 1000 °C and 21 MPa. A C/C composite (50 vol.% fibers, 33 vol.% carbon matrix, 5 vol.% ceramic–carbon hybrid and 12% porosity) exhibiting flexural strength 290 MPa, modulus 55 GPa and

toughness 2.9 MPa is obtained by hot-press pyrolysis in the presence of mesophase pitch powder, which serves as an additional binder, without densification after the pyrolysis. With the hybrid incorporation, the fiber content decreases from 53 to 50 vol.%, but the flexural strength and modulus are increased by 46% and 14% respectively, relative to the composite without the hybrid but with densification. This means that densification may be eliminated by the incorporation of the ceramic–carbon hybrid. The carbon in the hybrid has true density 1.7 g/cm^3, in contrast to the density of 1.3 g/cm^3 for the carbon matrix derived from the pitch.

The corresponding composite without the ceramic–carbon hybrid (without densification) contains 53 vol.% fibers and 37 vol.% carbon matrix (with the porosity excluded) and 10 vol.% porosity. The corresponding composite without the hybrid but with densification contains 54 vol.% fibers and 36 vol.% carbon matrix (with the porosity excluded) and 10 vol.% porosity. In spite of the increase in porosity upon hybrid incorporation, the thermal stability is improved. In spite of the decrease in fiber volume fraction upon hybrid incorporation, the flexural strength and modulus are increased by 64% and 46% respectively relative to the composite without hybrid or densification, and by 25% and 0% respectively relative to the composite without the hybrid but with densification (which entails 1 cycle of impregnation-carbonization). By scaling the properties to the values for the fiber volume fraction (50%) in the composite containing the hybrid, the hybrid incorporation increases the strength and modulus by 74% and 55% respectively relative to the composite without the hybrid or densification, and by 35% and 10% respectively relative to the composite without the hybrid but with densification. The significant strengthening provided by the hybrid incorporation is partly because the hybrid is also a binder. The extent of fiber pull-out on the fracture surface is much reduced by the hybrid incorporation. The true density is essentially not affected by the hybrid incorporation.

Alone, in the absence of any other ingredient, the ceramic–carbon hybrid can serve as a high-temperature structural monolith, due to the combination of filler and binder functions in the organoclay, its parent. Hot pressing the organoclay particles alone forms a black monolithic sheet with high thermal stability, electrical resistivity $6 \times 10^6\ \Omega$ cm, flexural strength 180 MPa, modulus 69 GPa, low ductility and weight loss at 800 °C being 0.08%. In the absence of an organic component, the clay particles, upon hot pressing, also forms a monolithic sheet, but the flexural strength and modulus, toughness and thermal stability are lower, though the ductility is higher. This means that both the organic component and the inorganic component of the organoclay contribute to causing the binding of the hot-pressed material. Without the organic component, the binding ability is less.

Acknowledgement

The authors thank Mr. Brian Schultz, Dr. Shoukai Wang and Mr. Mark Lukowski of University at Buffalo, State University of New York, for technical assistance.

REFERENCES

[1] Koo JH, Lao SC, Jor HK, Pilato LA, Wissler GE, Lee J et al. Thermo-oxidative studies of nanomodified carbon/carbon composites. Proc. American Society for Composites, Technical Conference, vol. 22nd. 2007. p. 117/1–117/20.
[2] Lin J, Ma CM, Tai N, Wu W, Chen C. Preparation and properties of SiC modified carbon/carbon composites by carbothermal reduction reaction. J Mater Sci Lett 1999;18:1353–5.
[3] Kowbel W, Bruce C, Withers JC, Ransome PO. Effect of carbon fabric whiskerization on mechanical properties of C–C composites. Compos A 1997;28A:993–1000.
[4] Cai Y, Fan S, Liu H, Zhang L, Cheng L, Jiang J, et al. Mechanical properties of a 3D needled C/SiC composite with graphite filler. Mater Sci Eng A 2010;527:539–43.
[5] Ko T, Kuo W, Han W, Day T. Modification of a carbon/carbon composite with a thermosetting resin precursor as a matrix by the addition of carbon black. J Appl Polym Sci 2006;102:333–7.
[6] Xiao P, Lu X, Liu Y, He L. Effect of in situ grown carbon nanotubes on the structure and mechanical properties of unidirectional carbon/carbon composites. Mater Sci Eng A 2011;528:3056–61.
[7] Jain R, Vaidya UK, Haque A. Processing and characterization of carbon–carbon nanofiber composites. Adv Compos Mater 2006;15(2):211–41.
[8] Giese RF, van Oss CJ. Organophilicity and hydrophobicity of organoclays. In: Yariv S, Cross H, editors. Organo–clay complexes and interaction. New York: Dekker; 2002. p. 175–222.
[9] Chan M, Lau K, Wong T, Ho M, Hui D. Mechanism of reinforcement in a nanoclay/polymer composite. Compos: Part B 2011;42:1708–12.
[10] Khan SU, Munir A, Hussain R, Kim J. Fatigue damage behaviors of carbon fiber-reinforced epoxy composites containing nanoclay. Compos Sci Technol 2010;70:2077–85.
[11] Lin C, Chung DDL. Nanoclay paste as thermal interface material for smooth surfaces. J Electron Mater 2008;37(11):1698–709.
[12] Hatta H, Suzuki K, Shigei T, Somiya S, Sawada Y. Strength improvement by densification of C/C composites. Carbon 2001;39:83–90.
[13] Chung DDL. Carbon fiber composites. Boston: Butterworth-Heinemann; 1993.
[14] Callister Jr WD, Rethwisch DG. Materials science and engineering: an introduction. 8th ed. Hoboken: Wiley; 2009. p. A5–A6.
[15] Chu Y, Fu Q, Li H, Li K. Thermal fatigue behavior of C/C composites modified by SiC–$MoSi_2$–$CrSi_2$ coating. J Alloys Compd 2011;509:8111–5.
[16] Michalowski J, Mikociak D, Konsztowicz KJ, Blazewicz S. Mechanical properties of C/C composites processed by wet impregnation and P-CVI methods. J Mater Sci 2011;46:5587–94.
[17] Wang S, Chung DDL. Self-sensing of flexural strain and damage in carbon fiber polymer–matrix composite by electrical resistance measurement. Carbon 2006;44(13):2739–51.
[18] Callister Jr WD, Rethwisch DG. Fundamental of materials science and engineering. 3rd ed. Hoboken: Wiley; 2008. p. 806 and 812.
[19] Serrano FJ, Bastida J, Amigo JM, Sanz A. XRD line broadening studies on mullite. Cryst Res Technol 1996;31(8):1085–93.

[20] Albuquerque FR, Parente1 B, Lima SJG, Paskocimas CA, Longo E, Souza AG, et al. Thermal transformations of tile clay before and after kaolin addition. J Therm Anal Calorim 2004;75:677–85.
[21] Reich S, Thomsen C. Raman spectroscopy of graphite. Philos Trans R Soc London A 2004;362:2271–88.
[22] Montilla F, Morallón E, Vázquez JL, Alcañiz-Monge J, Cazorla-Amorós D, Linares-Solano A. Carbon–ceramic composites from coal tar pitch and clays: application as electrocatalyst support. Carbon 2002;40(12):2193–200.
[23] Goswami R, Chakravartty SC, Krishna JBM, Bose E, Das D, Chaudhury SK, et al. AC conductivity and dielectric analysis of graphite–clay nanocomposite. Can J Phys 2011;89:1255–60.
[24] Park H, Kweon D, Lee J. The effect of SiC codeposition on the structure and mechanical properties of carbon/carbon composites prepared by chemical vapor deposition. Carbon 1992;30(6):939–41.
[25] Kim Y, Lee J. The effect of SiC codeposition on the oxidation behavior of carbon/carbon composites prepared by chemical vapor deposition. Carbon 1993;31(7):1031–8.
[26] Mentz J, Müller M, Buchkremer HP, Stöver D. Carbon-fibre-reinforced carbon composite filled with SiC particles forming a porous matrix. Mater Sci Eng A 2006;425(1–2):64–9.
[27] Gao NF, Kume S, Watari K. Zeolite–carbon composites prepared from industrial wastes: (I) effects of processing parameters. Mater Sci Eng A 2005;399(1–2):216–21.
[28] Gao NF, Kume S, Watari K. Zeolite–carbon composites prepared from industrial wastes: (II) evaluation of the adaptability as environmental materials. Mater Sci Eng A 2005;404(1–2):274–80.
[29] Ma J, Tan J, Du X, Li R. Effects of preparation parameters on the textural features of a granular zeolite/activated carbon composite material synthesized from elutrilithe and pitch. Microporous Mesoporous Mater 2010;132(3):458–63.
[30] Brunton GD. Density and compressibility of Wyoming bentonite particles. Clays Clay Miner 1988;36(1):94–5.
[31] Kamble R, Ghag M, Gaikawad S, Panda BK. Halloysite nanotubes and applications: a review. J Adv Sci Res 2012;3(2):25–9.
[32] Zaia DAM. Adsorption of amino acids and nucleic acid bases onto minerals: a few suggestions for prebiotic chemistry experiments. Int J Astrobiol 2012;11(4):229–34.
[33] Koegel-Knabner I, Guggenberger G, Kleber M, Kandeler E, Kalbitz K, Scheu S, et al. Organo-mineral associations in temperate soils: integrating biology, mineralogy, and organic matter chemistry. J Plant Nutr Soil Sci 2008;171(1):61–82.
[34] Basile-Doelsch I, Brun T, Borschneck D, Masion A, Marol C, Balesdent J. Effect of landuse on organic matter stabilized in organomineral complexes: a study combining density fractionation, mineralogy and δ 13C. Geoderma 2009;151(3–4):77–86.